URSI GASS 2023, Sapporo, Japan, 19 – 26 August 2023

Radio-Frequency Dosimetry of in vivo Experiments with Aquatic Larval Yellow Fever Mosquitoes

Eline De Borre*[(1)] and Arno Thielens [(1)]
(1) Ghent University - Imec, Department of Information Technology, Ghent, Belgium; e-mail: eline.deborre@ugent.be; arno.thielens@ugent.be

Abstract

Numerical simulations were conducted as a dosimetric study for in vivo exposure experiments. The experiments will use a frequency of 3.6 GHz and an incident electric field strength of 61 V/m to expose Yellow Fever mosquitoes (*Aedes aegypti*), a vector for multiple diseases, in the larval stage to examine the influence of radio frequency electromagnetic fields (EMFs) on the development of this model organism. The larval stage is aquatic, therefore Petri dishes of 3.5 cm diameter were used wherein the larvae were placed in different positions in the Finite Difference Time Domain simulations. A larva that is breathing at the surface, will experience more EMF power absorption compared to a larva eating near the bottom of the dish, for all four sizes (instars) of the *Ae. aegypti* larva. In the real exposure experiments, multiple Petri dishes will be exposed at the same time. Extra simulations were added with 168 Petri dishes, that indicate that the most power absorption by water will happen at the corners of the system compared to the Petri dishes in the middle.

1 Introduction

Yellow Fever mosquitoes (*Aedes aegypti*) are part of ecosystems, pollinate plants and most importantly, are vectors for diseases such as Dengue, Zika and Yellow Fever. [1] This species is found mostly near humans as the females prefer to feed on human blood. [2] Hence, they are often exposed to anthropogenic electromagnetic fields (EMFs). The effects of radio-frequency (RF)-EMFs on insects however is not yet widely studied. Regarding mosquitoes, the current literature is limited. The development of this insect under RF-EMF exposure has not yet been investigated. However, due to its ecological and health-related relevance and due to the existence of well-defined protocols for rearing this species, our aim is to use A. aegypti as a model organism for developmental effects of RF-EMF exposure of insects.

More specifically, we aim to study the development of this species when exposed to 3.6 GHz, a frequency related to 5G-NR telecommunication networks that are currently being rolled out. Our final goal is to execute an experiment on larvae, an aquatic life stage, in an RF-EMF reverberation chamber (RC). The larva goes through four instars phases during the larval stage that should be accounted for, with instar 1 being the smallest and instar 4 the largest. [4] In order to correctly interpret these experiments, the insects' dose needs to be determined. This can be done using numerical simulations of mosquito larvae exposed to RF-EMFs. These simulations have two goals: (1) quantify the spread of the dosage over the studied mosquito populations and (2) to link the targeted electric field strengths in the RC to dosages of the larvae. The former goal is studied by running simulations that assess the influence of the larval instar, the position of the larvae, and possible shielding effects on the dosage. These simulations are done for an electric field strength of 1 V/m. To reach the second goal, the results can be scaled to the targeted field strengths for the RC.

2 Method

The simulations were done using Finite difference time domain (FDTD) in Sim4Life (ZMT, Zurich, Switzerland) for 12 plane waves with different incident angles and polarizations as can be seen in Figure 1. From the simulation, the whole-body power absorption (P_{abs}) will be computed for the larvae:

$$P_{abs} = \int \sigma \times |\vec{E}_{int}|^2 \cdot dV, \qquad (1)$$

with σ the conductivity, $|\vec{E}_{int}|$ the root mean square internal electric field strength and V the volume of the larva. [3]

The FDTD method is often used as a simulation technique for dosimetric studies in EMF exposure situations and has been used for simulations for in vivo [5-7] and in vitro [8] experiments in an RC. First, the electric field (EF) strength is established, followed by far field plane wave simulations. [6,7]. The time averaged EF strength is assumed to be constant over the working volume in an unloaded condition, we will use an EF strength of 1 V/m for the simulations, which later can be rescaled. Second, the FDTD simulations for different incident AoA are conducted and the average is taken. We assume that the average P_{abs} can be taken over multiple plane wave simulations, instead of computing the multipath exposure. [6] The 12 different incident angles were chosen as in [9,10] and are expected to result in P_{abs} that span all possible P_{abs}, if the larva would be in free space. These incident plane waves are orientated along the main axes of the spheroid model in the horizontal and vertical positions.

The larvae will be placed in Petri dishes with a diameter of 3.5 cm during the experiment, and thus the simulations will include the water (9.15 mm height) and the Petri dish. First, a sole Petri dish will be considered in different situations. The larvae were modeled as spheroids, based on their average dimensions [4], the major axis is taken as the length of the insect and the minor axis is taken as the width of the head. Due to the large difference in size for the instars of the larvae, simulations were done on all four instars separately. Three different forms of spatial orientation and position of the larvae in the Petri dishes are considered as shown in Figure 1: major axis along the z-axis in the middle of the dish and one end at the surface (vertical), the same position but with a 30° angle from the z-axis (tilted), and major axis along the x-axis near the bottom of the dish (horizontal). In the real exposure situation during the experiment, the Petri dishes are placed in four levels with 6 columns and 7 rows, with 6.4 cm between the levels. Therefore, simulations with these 168 dishes were also considered, without larvae for a lower computational time.

The frequency in all simulations was 3.6 GHz, however extra simulations were also done for 6, 12, 24 and 60 GHz with vertical larva position. Some symmetry meant that not all 12 simulations were needed in all cases, however the 12 configurations were always accounted for when the mean was taken of the different directions. The voxel size of the spheroids was set to 0.05 mm and of the water to 0.3 mm, these voxels are made sure to be < 1/10 of the wavelength in the medium [11]. The dielectric properties of the larvae were based on the measurements of adult *A. aegypti* dielectric measurements [3]. The dielectric properties of the larvae are taken as 10% of water and 90% of the adult dielectric properties. [12]

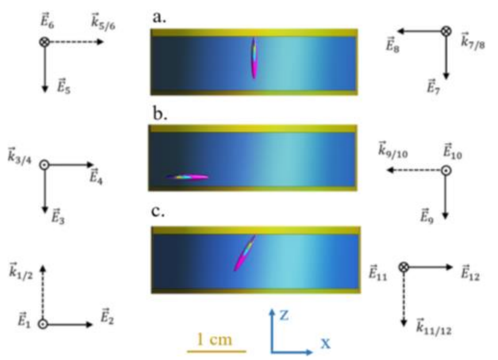

Figure 1. Larval positions in simulations and incident and polarization angles of the 12 incident plane waves and the four different instars **a.** Vertical position, **b.** Horizontal position, **c.** Tilted position.

To compare these compositions and frequencies, a root mean square (RMS) value of EF strength of 1 V/m was used. The targeted incident EF strength of the experiment is 61 V/m, this EF strength was chosen based on the ICNIRP (International Commission on Non-Ionizing Radiation Protection) reference level for the 30-minute whole-body average, for a uniform plane wave. [13] The P_{abs} results of the 1 V/m simulations can be scaled to account for experiments with different EF strengths [14,15] in the following way:

$$P_{abs,new} = \frac{E_{RMS}^2}{1\,V^2/m^2}\, P_{abs,1V/m}, \qquad (2)$$

with $P_{abs,new}$ the whole-body power absorption when exposed to an EF strength of E_{RMS} and $P_{abs,1V/m}$ the whole-body power absorption when exposed to an incident EF strength of 1 V/m.

3 Results and Discussion

3.1 Instar and frequency dependency

A difference in size between the instars, will lead to a difference in P_{abs}, shown in Figure 2.a for the vertical position, different frequencies and an incident EF strength of 1 V/m. In the first day of the experiment, the larvae will be instar 1, the whole-body power absorption will be lower than for the later instars. If we look at the absorbed power normalized to its volume, the difference between the different instars is relatively small for 3.6 and 6 GHz, shown in Figure 2.b. However, this is not the case for higher frequencies, here the smaller the instar, the more power absorbed when normalized to the volume.

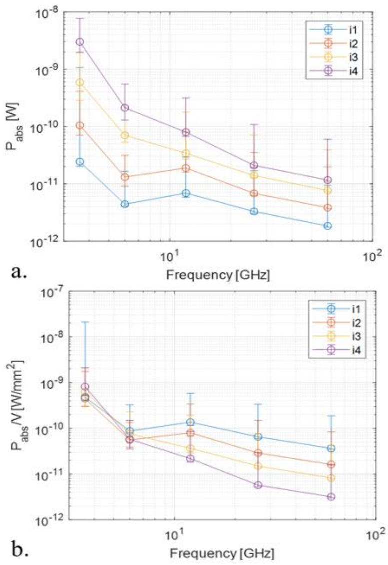

Figure 2. a. Whole-body averaged absorbed power and **b.** average absorbed power divided by the volume of the spheroids, of the 12 plane wave simulations of the 4 larval instars (i1, i2, i3 and i4) in vertical position for an incident field strength of 1 V/m in a Petri dish with 3.5 cm diameter, as function of frequency. The bars indicate the minimum and maximum of the 12 different plane wave simulations.

The experiment will use a frequency of 3.6 GHz, the absorbed power over the small volume of the insect is similar for the different instars, so the influence of the instar in the exposure experiment is expected to be neglectable.

3.2 Influence of Larval Position within the Petri Dish

Larvae are often found at the bottom of the Petri dish to look for food (horizontal position) or at the surface to breath (vertical and tilted position). A difference between these positions will also lead to a difference in power absorption as can be seen in Table 1. In this table, the mean of P_{abs} for the 12 simulations for the four instars and the three positions are given, together with the maximum and minimum P_{abs} of the 12 simulations. For instar 3, formula (2) was used to show values for the targeted 61 V/m.

Table 1. Mean, min. and max. of the absorbed powers in [W], of the larvae for the 12 incident angles, in different positions and instars at 3.6 GHz at 1 V/m, and for instar 3 also at 61 V/m.

Instar		i1	i2	i3	i4	i3
	EF	1 V/m	1 V/m	1 V/m	1 V/m	61 V/m
Vertical	Mean P_{abs}	2.44 x 10^{-11}	1.05 x 10^{-10}	5.89 x 10^{-10}	3.00 x 10^{-9}	2.19 x 10^{-6}
	Min.	2.44 x 10^{-11}	3.43 x 10^{-11}	3.05 x 10^{-10}	1.04 x 10^{-9}	1.13 x 10^{-6}
	Max.	2.44 x 10^{-11}	3.09 x 10^{-10}	1.39 x 10^{-9}	4.71 x 10^{-9}	5.15 x 10^{-6}
Horizontal	Mean P_{abs}	7.67 x 10^{-12}	3.32 x 10^{-11}	1.39 x 10^{-10}	5.93 x 10^{-10}	5.18 x 10^{-7}
	Min.	2.60 x 10^{-12}	1.20 x 10^{-11}	3.62 x 10^{-11}	2.24 x 10^{-10}	1.35 x 10^{-7}
	Max.	1.40 x 10^{-11}	5.72 x 10^{-11}	3.57 x 10^{-10}	2.11 x 10^{-9}	1.33 x 10^{-6}
Tilted	Mean P_{abs}	2.37 x 10^{-11}	9.46 x 10^{-11}	4.31 x 10^{-10}	2.17 x 10^{-9}	1.60 x 10^{-6}
	Min.	4.95e x 10^{-12}	1.94 x 10^{-11}	1.92 x 10^{-10}	5.12 x 10^{-10}	7.13 x 10^{-7}
	Max.	7.12 x 10^{-11}	2.76 x 10^{-10}	1.01 x 10^{-9}	3.86 x 10^{-9}	3.74 x 10^{-6}

When the P_{abs} are normalized over the volumes of the larva spheroids (instar 1: 0.051 mm², instar 2: 0.237 mm², instar 3: 0.934 mm², instar 4: 3.676 mm²), a similar result is again found for the four instars for the horizontal and tilted position. However, there is a difference between the positions. When the larvae are looking for food near the bottom (horizontal), they will experience less power absorption than when they go to the surface for air (vertical and tilted) due to its position in the water. The surrounding water will also interact with and absorb the EMFs. The highest power absorption of the larvae will happen for the vertical position. During the experiment, an EF strength of 61 V/m will be used, the related P_{abs} can be found in the last column of Table 1. These values are considerably larger, 3721 times higher, than for the 1 V/m.

3.3 Multiple Petri Dishes

In the more realistic simulations with 168 dishes, not all Petri dishes experience the same power absorption of the water. An empty RC will provide a uniform exposure within the working volume [6], in a loaded RC the position can be of importance [16].

When the results of the twelve angles of incidence are averaged, there is still a difference in power absorption depending on the Petri dishes position. The positions with the lowest P_{abs} by the water in the Petri dish are on the 2nd and 3rd level in column 2 and 5, in row 4, with a P_{abs} of 393 µW. The positions with highest P_{abs} by the water in the Petri dish are at the 8 corners of the exposed system, i.e. level 1 and 4, column 1 and 6 and row 1 and 7. The P_{abs} at these corners are 1303 µW. Note that these results are based on the mean of the 12 plane waves that have an incident angle horizontal or vertical along the tray levels, which were chosen because extreme results in P_{abs} are expected compared to random angles, and that the P_{abs} are computed for the water and not for larvae. It is expected that when the water of a Petri dish experiences a shielding effect, this will also effect the power absorption of the larva in the Petri dish to some degree. Displacements of the Petri dishes are also expected to have an influence of this shielding effect. In general, the dishes at the sides of the system have a higher P_{abs} than the ones in the center due to a shielding effect. This implies that when observations are made in the in vivo experiment, the Petri dishes can be categorized in respect with the positions with more or less power absorption. Or, alternatively, the experiment protocol can include a rotation on position of the Petri dishes within the RC. The relative differences are small between the Petri dishes (max. 107%), it is expected that difference in dose between the Petri dishes with the lowest dose in the exposed experiment and the sham exposed dishes will be much higher (> factor 1000) than the differences within the exposed categories.

5 Conclusion

A dosimetric study was done by means of numerical simulations, for a setup that will be used in exposure experiments of *Ae. aegypti* larvae, an aquatic life stage. The whole-body absorbed power was found to be similar for all sizes (instars) of the larvae in a Petri dish, when normalized to their volume for a frequency of 3.6 GHz, and so the influence of the size is small. When a frequency of 12 GHz or higher is used, the smaller larvae will have higher power absorption compared to the larger larvae when normalized for their volume. A difference in position of the larvae in the Petri dish, will result in a different dose. A larvae that is looking for food at the bottom, will experience less power absorption than a larvae looking for air at the surface. The exposure of the experiment was chosen to be around 61 V/m at 3.6 GHz. During the experiment, multiple Petri dishes will be exposed. In this case, a difference in power absorption can occur depending on the relative position of the Petri dish. To account for these differences, a rotation protocol for the Petri dishes can be applied during the experiment.

Acknowledgements

This work was funded by the Research Foundation Flanders (FWO) under grant agreement no. G033220N. Arno Thielens is a postdoctoral fellow of the Research Foundation Flanders (FWO) under grant agreement no. 1283921N.

References

[1] J. Reinhold, C. Lazzari, and C. Lahondère, “Effects of the environmental temperature on Aedes aegypti and aedes albopictus mosquitoes: A Review*,” Insects*, **9**, 4, p. 158, Nov. 2018, doi:10.3390/insects9040158.

[2] S. A. Khan, A. Ombugadu, and S. Ahmad, “Host-seeking behavior and fecundity of the female aedes aegypti to human blood types,” *Pest Management Science*, **78**, 1, pp. 321–328, Sep. 2021, doi:10.1002/ps.6635.

[3] E. De Borre, W. Joseph, R. Aminzadeh, P. Müller, M. N. Boone, I. Josipovic, S. Hashemizadeh, N. Kuster, S. Kühn, and A. Thielens, “Radio-frequency exposure of the yellow fever mosquito (A. Aegypti) from 2 to 240 GHz,” *PLOS Computational Biology*, **17**, 10, Oct. 2021, doi: 10.1371/journal.pcbi.1009460.

[4] A. Bar, and J. Andrew, “Morphology and morphometry of Aedes aegypti larvae,” *Annual Research & Review in Biology*, **3**, 1, pp. 1-21, Feb. 2013.

[5] T. Wu, A. Hadjem, M.-F. Wong, A. Gati, O. Picon, and J. Wiart, “Whole-body new-born and Young Rats' exposure assessment in a reverberating chamber operating at 2.4 GHz,” *Physics in Medicine and Biology*, **55**, 6, pp. 1619–1630, Feb. 2010, doi:10.1088/0031-9155/55/6/006.

[6] R. Ito, S. Jeon, J. Wang, A. Lee, J. Pack, H. Choi 1, Y. H. Ahn, and K. Imaida, “Quantification of Exposure Level in a Reverberation Chamber for a Large-Scale Animal Study,” *IEEE Journal of Microwaves*, **2**, 3, July 2022, pp. 522-532, doi: 10.1109/JMW.2022.3176283.

[7] J. Shi, J. Chakarothai, J. Wang, K. Wake, S. Wanatabe, and O. Fujiwara, “Quantification and verification of whole-body-average SARS in small animals exposed to electromagnetic fields inside reverberation chamber,” *IEICE Transactions on Communications*, **E97.B**, 10, pp. 2184–2191, 2014, doi: 10.1587/transcom.e97.b.2184.

[8] R. Orlacchio, G. Andrieu, A. Joushomme, L. Patrignoni, A. Hurtier, F. P. De Gannes, I. Lagroye, Y. Percherancier, D. Arnaud-Cormos, and P. Leveque, “A novel reverberation chamber for in vitro Bioelectromagnetic experiments at 3.5 GHz,” *IEEE Transactions on Electromagnetic Compatibility*, pp. 1–12, Dec. 2022, doi: 10.1109/temc.2022.3216045.

[9] A. Thielens, D. Bell, D. B. Mortimore, M. K. Greco, L. Martens, and W. Joseph, “Exposure of insects to radio-frequency electromagnetic fields from 2 to 120 ghz,” *Scientific Reports*, **8**, 1, Mar. 2018, doi:10.1038/s41598-018-22271-3.

[10] C. R. Bhatt, A. Thielens, B. Billah, M. Redmayne, M. J. Abramson, M. R. Sim, R. Vermeulen, L. Martens, W. Joseph, and G. Benke, “Assessment of personal exposure from radiofrequency-electromagnetic fields in Australia and Belgium using on-body calibrated exposimeters,” *Environmental Research*, **151**, pp. 547–563, Nov. 2016, . doi:10.1016/j.envres.2016.08.022.

[11] J. W. Hand, “Modelling the interaction of electromagnetic fields (10 mhz–10 ghz) with the human body: Methods and applications,” *Physics in Medicine and Biology*, **53**, 16, 2008, doi:10.1088/0031-9155/53/16/r01.

[12] R. Massa, M. D. Migliore, G. Panariello, D. Pinchera, F. Schettino, E. Caprio, and R. Griffo, “Wide band permittivity measurements*of palm*(phoenix canariensis)*and*rhynchophorus ferrugineus (Coleoptera Curculionidae)*for RF pest control*,” *Journal of Microwave Power and Electromagnetic Energy*, **48**, 3, pp. 158–169, May 2014, doi:10.1080/08327823.2014.11689880.

[13] International Commission on Non-Ionizing Radiation Protection. "Guidelines for limiting exposure to electromagnetic fields (100 kHz to 300 GHz)." *Health physics*, **118.5**, pp. 483-524, 2020.

[14] A. Thielens, M. K. Greco, L. Verloock, L. Martens, and W. Joseph, “Radio-frequency electromagnetic field exposure of Western Honey Bees,” *Scientific Reports*, **10**, 1, Jan. 2020, doi:10.1038/s41598-019-56948-0.

[15] I. Liorni, M. Capstick, L. van Wel, J. Wiart, W. Joseph, E. Cardis, M. Guxens, R. Vermeulen, and A. Thielens, “Evaluation of specific absorption rate in the far-field, near-to-far field and near-field regions for Integrative Radiofrequency Exposure Assessment,” *Radiation Protection Dosimetry*, **190**, 4, pp. 459–472, Sep. 2020. 10.1093/rpd/ncaa127.

[16] J. B. Coder, J. M. Ladbury, C. L. Holloway, and K. A. Remley, “Examining the true effectiveness of loading a reverberation chamber: How to get your chamber consistently loaded,” *2010 IEEE International Symposium on Electromagnetic Compatibility*, Feb. 2010, doi:2010.10.1109/isemc.2010.5711332.